Reversible nanogate system for Mesoporous Silica Nanoparticles based on Diels-Alder adducts.

Rafael R. Castillo[a,b]*, David Hernández-Escobar[a]†, Sergio Gómez-Graña[a], María Vallet-Regí[a,b,c]*

The implementation of nanoparticles as nanomedicines require from sophisticated surface modifications in order to reduce immune response and enhance recognition abilities. In addition to that, Mesoporous Silica nanoparticles present extraordinary host-guest abilities and facile surface functionalization. These two factors make them ideal candidates for the development of novel drug delivery systems, at the expense of increasing the structural complexity. With this idea in mind, a system of triggerable and tunable silica nanoparticles was developed for its application as drug delivery nanocarriers. For that purpose, Diels-Alder cycloaddition adducts were chosen as thermal-responsive units; that permitted to bind Au nanocaps able to block the pores and allow the incorporation of targeting fragments. The capping efficiency was tested under different thermal conditions, obtaining outstanding efficiencies within the physiological range and mild temperatures, as well as enhanced releases under pulsing heating cycles which showed the best release profiles.

Introduction

The use of nanomedicine in novel medical approaches is one of the most promising methods to face advanced disease treatments with special complexity such as cancer.[1] Unfortunately, the reality is that current nanomedicine technology has not been able to completely overcome the use of conventional chemotherapeutics.[2,3] In the last decade, Mesoporous Silica Nanoparticles (MSNs) have attracted great attention in this regard due to a unique mesoporous structure able to retain small molecules like chemotherapeutics, but also because of their high biocompatibility,[4–6] slow biodegradability[7,8] and ease of functionalization. All these features, quickly positioned this material as a valuable platform for the development of stimuli-responsive drug delivery systems.[9-12] Nevertheless, in order to become feasible as nanomedicines, MSNs require a series of surface modifications. Ideal functionalized MSNs would be able to limit the immune response, augment bloodstream circulation time[13,14] provide vectorization abilities[15] and create responsive gating systems able to prevent undesired leakages.[16,17] Despite the fact that the current gating nanotechnology is based on complex chemical modifications, rising costs and often making these systems unattractive for pre- and clinical trials, we firmly believe that the advantages outweigh the disadvantages.

[a] Dpto. Química en Ciencias Farmacéuticas. Facultad de Farmacia, Universidad Complutense de Madrid. (Plaza Ramón y Cajal s/n, 28040, Madrid, Spain).Email: R. R. Castillo: rafcas01@ucm.es; M. Vallet-Regí: vallet@ucm.es Fax: +34913941786
[b] Centro de Investigación Biomédica en Red (CIBER).
[c] Instituto de Investigación Sanitaria Hospital 12 de Octubre (i+12)
† Dept. of Chemical Engineering and Materials Science, Michigan State University (East Lansing 48824, MI, USA).

Supporting information for this article is given via a link at the end of the document

Considering those limitations, we decided to explore a straightforward and quick strategy to develop gated nanohybrids with all the required features for drug delivery: stimulus responsiveness, stealthiness and vectorization abilities. In this work, MSNs and gold nanoparticles (AuNPs) were chosen, having this combination previously demonstrated a good stability and ease of functionalization.[18]

Particularly, AuNPs have been widely used in other biomedical disciplines such as nanotherapeutics[21-25] and gene monitoring/modulation devices for living cells.[23] Additionally, Au show great compatibility with the chosen thermosentitive moiety, which have been employed by Workentin and coworkers on studies dealing with cycloadditions onto gold nanoparticles[26, 27] and the development of AuNPs-based assemblies[28] and platforms throughout this type of reactions.[29]

In order to take advantage of both types of nanoparticles, the MSNs should be coated with AuNPs. This arrangement would block pore outlets to prevent the release of the payload while would also allow the anchoring of targeting elements easily. Similar strategies have been employed successfully, as reported in the literature, where the coating with AuNPs has been performed throughout electrostatic deposition,[30,31] cyclodextrin-adamantane supramolecular interaction,[32,33] acid-sensitive linker[34] or displaceable DNA sequences.[35] Notwithstanding with the above, all reported models suffer from a low Au to MSNs ratio which do not ensure efficient capping, as observed from the published TEM images. Moreover, none of them has been functionalized with vectoring moieties, what gives value to our model.

In our design, we have included a thermally breakable linking fragment based on Diels-Alder (DA) cycloaddition adducts, with well-known thermal properties as demonstrated on self-healing polymers,[36,37] polymer-based devices[38,39] and even silica particles.[40-42] However, none of these materials were designed to have biological applications. In contrast, the nanodevice here presented has outstanding biocompatibility, plus a clear vectorization ability. Moreover, we have also addressed retention and release studies of the prepared hybrids in order to fully demonstrate the operating mechanism, which we believe was poorly covered in previous examples.

Results and Discussion

As it has been outlined in the introduction, this work addresses the synthesis of MSN-Au hybrids employing Diels-Alder adducts as thermal responsive linkers for delivery platform. The construction of these nanomaterials was achieved throughout a stepwise procedure in which the DA adduct was built directly onto the surface of MSNs prior to the incorporation of the AuNPs (Figure 1). The starting amino capped MSNs prepared by a modified Stöber methodology (1.3 mmolNH_2/g MSN, Supporting Information) were reacted with the maleimidoglicine dienophile in DMF employing HOBt and HBTU as amide bond formation reagents. The maleimide functionalized MSNs (MSN-MalGly) were successfully transformed into the Diels-Alder modified MSNs (MSN-DA) after reaction with an excess of methylfurfuryldisulfide (MFD). The different reaction parameters: time, temperature and reagent excess were coarsely optimized

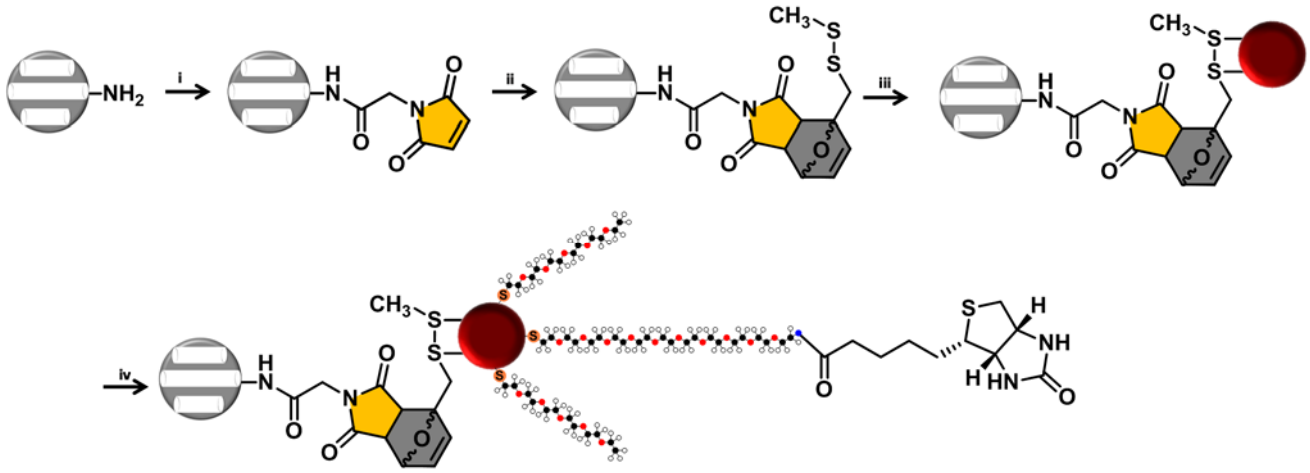

Figure 1: General synthetic scheme followed in the preparation of the biotin-targeted MSN-DA-Au hybrids. Reaction conditions: (i) MalGly (1.5equiv.) HOBt (3 equiv.), HBTU (2 equiv.), DIPEA (6 equiv.), RT, 24h, DMF; (ii) MFD (excess), MeCN, RT, 48h; (iii and iv) MSN-DA dropwise added over AuNPs folowed by capping with thiolated PEGs, H_2O, RT (see experimental procedure for additional details).

by determining the mass loss obtained for each batch. (Table S1) The best results were those which employed MeCN and 4 μL of MFD per silica milligram at RT during 48h. The successful functionalization was determined by both IR and thermogravimetric assays (Figures S1 to S4, Supporting information).

The ordered structure of the prepared nanoparticles was confirmed using small angle X-rays diffraction, showing the typical pattern for a MCM-41 porous structure and was maintained throughout all modifications (Figure S5). Pore width and volume varied as expected throughout the synthetic procedure according to the N_2 adsorption isotherm values obtained with the Brunnauer-Emmet-Teller (BET) approach (Figure 2). The data showed decreasing pore volume values as the functionalization increased, indicating higher constrainment at the pore outlet. The pore size distribution, according to BJH adsorption method provided a pore diameter of about 2.5 nm, suitable for hosting small molecules like conventional fluorescent probes and antiproliferative compounds.

The thermal behavior of MSN-DA was evaluated on aqueous based suspensions in order to simplify the translation into biocompatible environments. When tested in pure water or PBS, the MSN-DA showed poor colloidal stability due to quick aggregation and precipitation, together with a disfavored diene release consequence of its poor solubility. Therefore, to improve both the colloidal stability and solubility of the diene, reversibility assays were performed on a large volume of a DMSO/H_2O (1:4) for 72h at either 60ºC or 80ºC. Once heating was concluded, the particles were centrifuged, washed with ethanol and diethyl ether, and finally dried under vacuum at RT. These thermally treated MSNs were then analyzed by thermogravimetric analysis and FTIR (Figures S3, S4). Mass loss percentages and patterns and infrared adsorption bands were equivalent to the data obtained for MSN-MalGly, suggesting a complete retro Diels-Alder reaction. From the thermogravimetric assays, it is also noteworthy that the initial mass loss of MSN-DA between 200-300ºC seem to correspond to the expected region for dissociation-evaporation of MFD (Figure S2).

The adduct presence was evidenced too on solid ^{13}CNMR experiments (Figure S14) and when the particles were treated with citrate-stabilized colloidal Au. In this case the analysis by Transmission Electron Microscopy (TEM) of the resulting mixture showed the deposition of AuNPs onto MSNs' surface (Figure 3A). AuNPs were able to react spontaneously with the methyldisulfanyl group present on the surface of the MSN-DA, giving the MSN-Au hybrids, although the coating process under these circumstances was completely uncontrolled. To improve it, the dispersion of MSN-DA was added over an excess of colloidal Au. The first

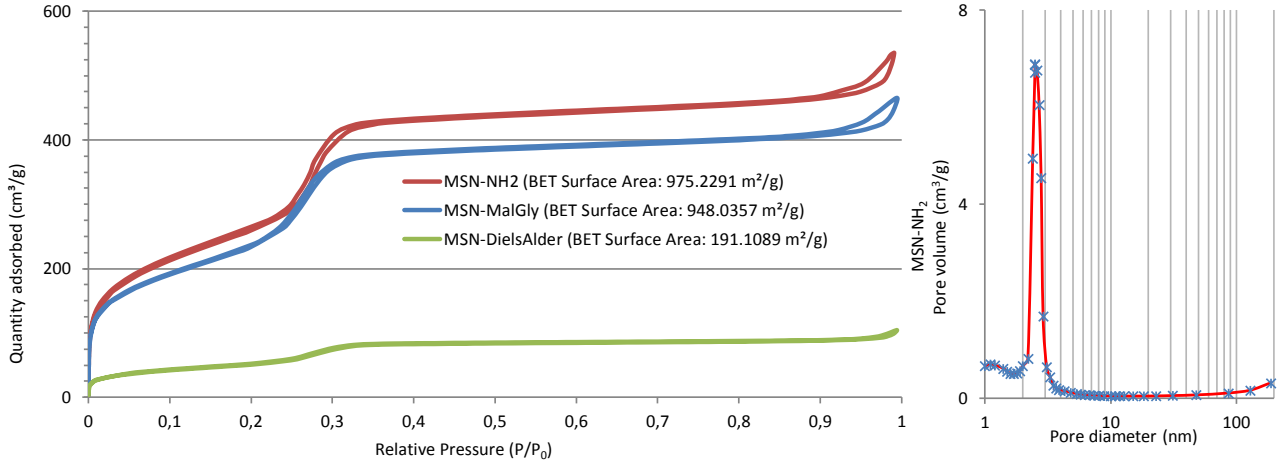

Figure 2: Comparative N_2 adsorption isotherms (BET) of prepared MSNs and their latter modifications. Pore size distribution (BJH) of the employed MSNs.

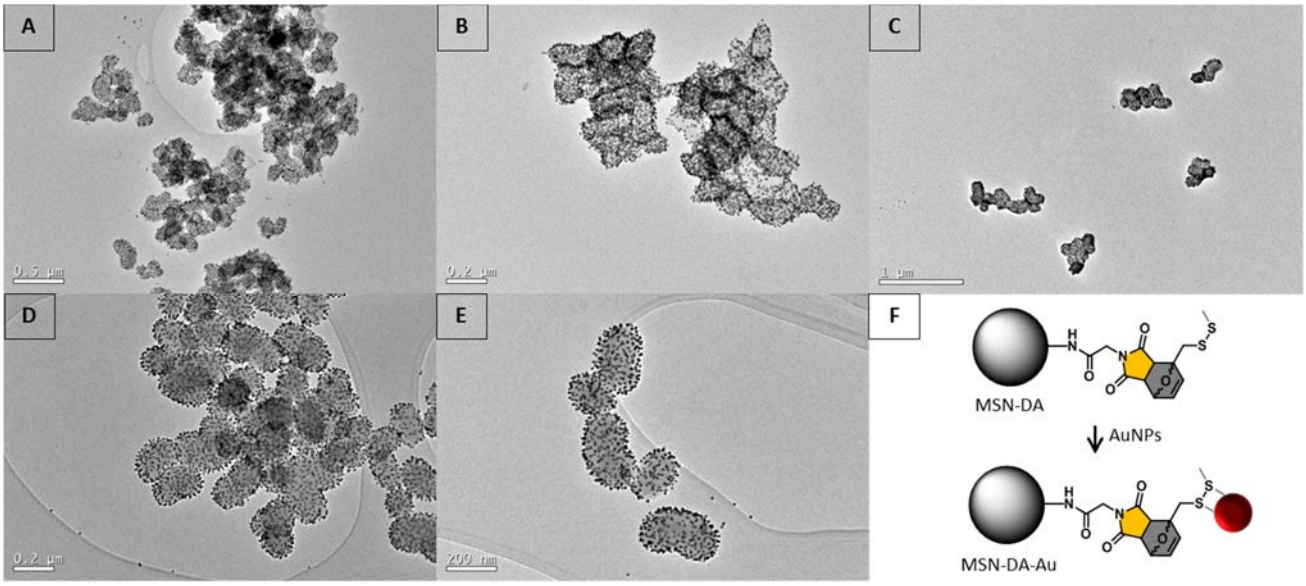

Figure 3: TEM micrographs of the different conditions tested for the preparation of MSN-DA-Au hybrids. (A) Au colloid: 0.5 mL/mg MSNs, 2h maturation, without sonication; (B) Au colloid: 0.5 mL/mg MSNs, 24h maturation, without sonication; (C) Au colloid: 1 mL/mg MSNs, 2h maturation, sonication; (D) Au colloid: 2 mL/mg MSNs, 2h maturation, without sonication; (E) Au colloid: 2 mL/mg MSNs, 0.5h maturation, sonication; (F) Scheme of the MSN-DA-Au nanohybrids formation. In all cases the final capping step with thiol containing PEG was done.

examples were carried out in water with 1 mg/mL of MSN-DA dropwise added over AuNPs. From these experiments it was found that at least 1 mL of Au colloid per milligrams of silica was necessary to obtain a homogeneous coating. Additionally, we could set the reaction time, observing the best results between 30 and 120 minutes. Under this conditions, it was observed that either a lower amount of AuNPs or longer reaction times produced again large aggregates. To fully optimize the coating process, an improved MSN-DA colloidal stability was required. This could be obtained modifying two conditions: first, with the use of an ultrasonic bath during the addition step and second, employing 1% of aqueous DMF as dispersant. The use of these two conditions allows to prepare hybrids with a low degree of aggregation, as observed in TEM micrographs. (Figure 3E) The formation of aggregates was prevented by the incorporation, a stabilizing thiolated-PEG (MW=800), which was added 10 minutes after the addition of MSN-DA. This step was effective in increasing the stability of the nanohybrids, up to 30 days, without significant variation on their hydrodynamic size. Purification step was performed by centrifugation (9000 rpm, 10', 10ºC), where the heavier MSN-DA-Au hybrids precipitated and the excess of colloidal Au, reagents and byproducts remained in the supernatant.

Dynamic-light scattering (DLS) analysis of the different MSNs showed hydrodynamic diameter values in the range of 300 nm for raw MSNs. Subsequent surface modifications did not alter substantially the size values according to DLS (Figure 4 and Figure S6). The final PEG-capped MSN-DA-Au hybrid showed extraordinary dispersibility in water although with a significant increase of size consequence of the incorporation of Au and PEG chains onto the MSNs' surface. Regarding the ξ-potential, a charge reversal was observed between the starting amino containing particles and their latter modifications MSN-MalGly and MSN-DA. Those values, which slightly differed from the expected neutral potentials, were consequence of the added DMF necessary to obtain optimal dispersion. On the MSN-DA-Au hybrids, the negative values recorded might be a consequence of remainder citrate. (Figure 4)

AuNPs have been broadly employed in biological applications because of their interesting optical properties.[43] Such optical properties are originated by the collective oscillation of conduction electrons when in resonance with the incoming light. This produces a light absorbance called localized surface plasmon resonance (LSPR).[44] Thanks to this physical feature, we were able to analyze by UV-Vis spectrometry both the capping efficiency and the fate of the AuNPs. In our model, this strategy was employed to determine the concentration of AuNPs retained onto the MSN hybrid (pellet) or released (supernatant) upon centrifugation after thermal breakdown conditions. Then, release experiments could be performed in water due to the outstanding colloidal stability of PEG-capped hybrids, which complemented the preliminary MSN-DA water-based reversibility studies of

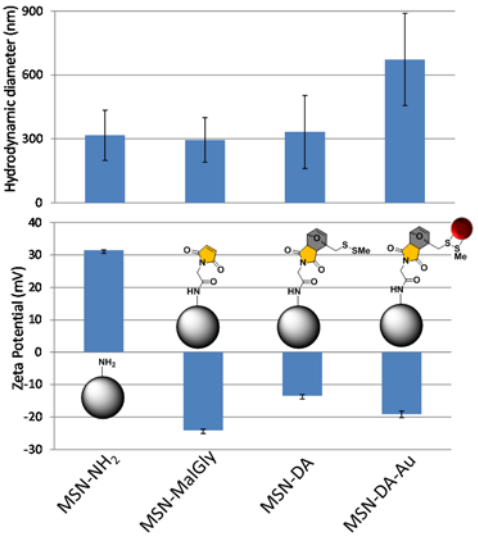

Figure 4: Hydrodynamic size (up) and ξ-potential (down) for MSNs and MSN-DA-Au. The measurements were recorded in 1% DMF in H_2O to obtain good dispersability for MalGly and Diels-Alder derivates. The data presented correspond to a mean of 5 measurements. Please see figure S6 in the Supporting Information for raw graphics.

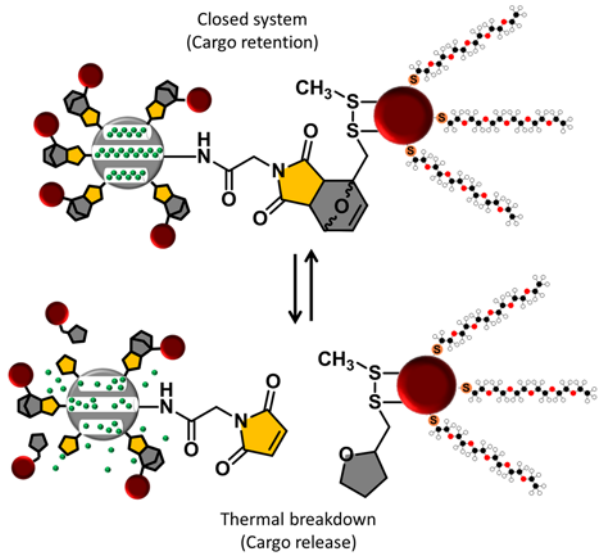

Figure 5: Plausible payload release mechanism of the MSN-DA-Au hybrids. The thermal induced retro Diels-Alder breakdown releases the capping AuNPs from the pore outlets, allowing the cargo diffusion.

MSN-DA (Supporting information). The thermal behavior of nanohybrids was studied by heating, a 100 µg/mL suspension of the prepared PEGylated MSN-DA-Au hybrid from RT to three different target temperatures 37, 65 and 90ºC. From each reaction, aliquots at 1, 2, 4, 24 and 48 hours were taken and centrifuged to separate the AuNPs (supernatant) from the MSN-DA-Au (pellet). The amount of AuNPs in each fraction was measured by UV-Vis observing that when mild temperatures were applied, most of the Au caps remained bound to the silica surface. (Figure 6). The constant values measured for free and bound AuNPs are in concordance with a release mechanism operated by a dissociation equilibrium. However, there is a divergent behavior in the case of harsh thermal treatments, (Figures S7 and S8 show the UV-Vis spectra of the released AuNPs at 90ºC.) which show a growing release of AuNPs during the first 4h followed by a significant concentration decrease of AuNPs in the supernatant between 24 and 48h. This effect could obey to aggregation processes that may take place between the released and retained AuNPs, as it is suggested by the shifting to higher λ values observed in the absorption of Au in the MSN-DA-Au pellet (Figures S7 and S8).

To demonstrate the postulated equilibrium-driven release, we decided to carry out a new set of *dynamic* heating experiments. On those, the hybrid was subjected to centrifugation after each heating cycle which permitted to separate the AuNP-diene fragment released from the decanted MSN-DA-Au hybrid. The recovered hybrid was then dispersed back with fresh medium and subjected again to thermal activation to set a new dissociation equilibrium. This resubmission to equilibrium produced a new partial cleavage of the DA, releasing more furan-AuNPs. The iterative repetition of this process would result in a net release of AuNPs greater than the obtained for single stage (*static*) thermal treatments.

As it is shown in Figure 7, the net AuNPs release is higher that the obtained from the previous conditions (*static* release conditions). For the experiment set at 37ºC, the UV-Vis spectra of the released AuNPs is negligible, meaning that practically no AuNPs were released from the MSN-DA-Au nanohybrid. However, on the 65ºC and 90ºC experiments, where the

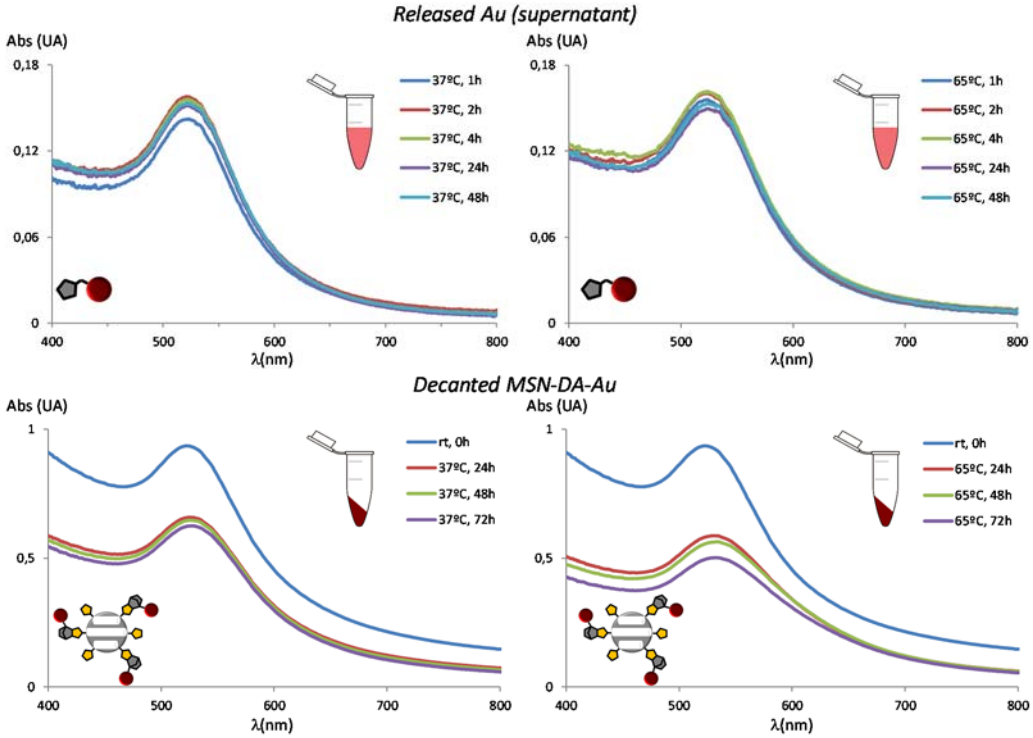

Figure 6: UV-Vis absorption spectra of gold nanoparticles released and retained in the silica from the thermal treated MSN-DA-Au hybrid. In this case the hybrids were subjected to a *static* thermal treatment during 72h period. For clarity, due to the poor information provided, data regarding Au detection on the recovered solid MSNs for 1, 2 and 4 h is not included. Data corresponding to supernatant Au detection at 72h is not included either. Please check figure S7 for data regarding the 90ºC experiment and figure S8 for comparative curves after the 72h heating period

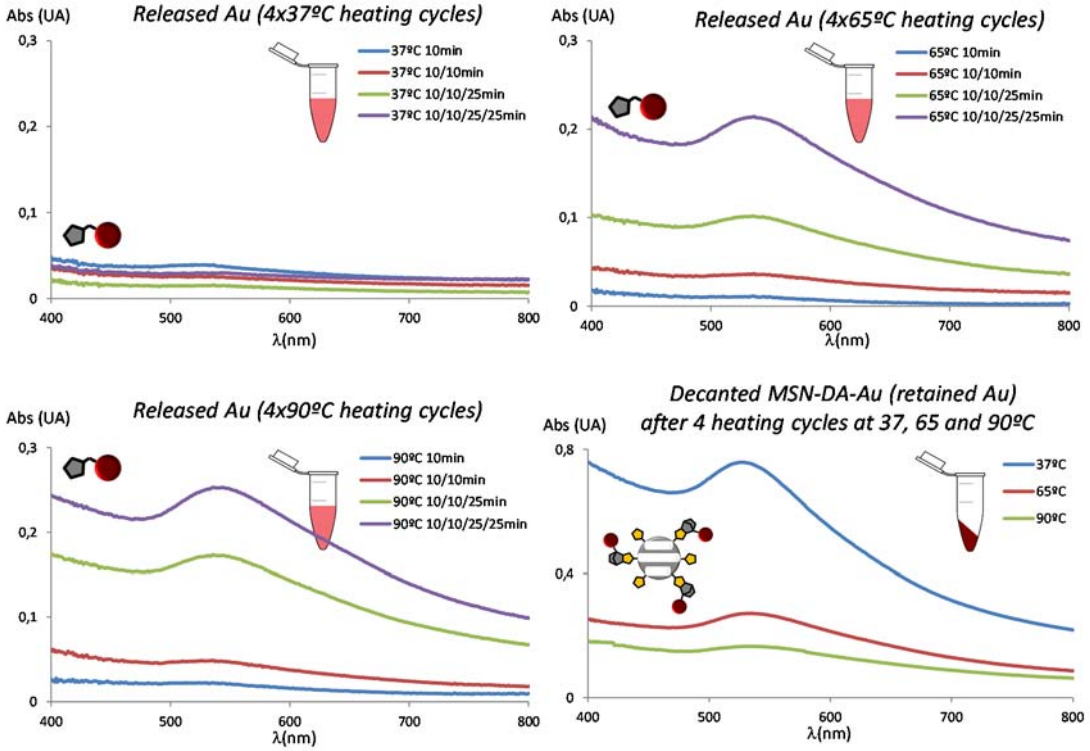

Figure 7: Absorption spectra of released and retained gold nanocaps from the hybrid MSN-DA-Au under "dynamic" thermal treatment. For actual pictures of the final dispersion of MSN-DA-Au nanohybrids after the cyclic treatment see figure S10. The time indications (10/10/25/25 and related) refer to the duration of each heating cycle to which the hybrid was submitted. Cooling down steps were iteratively introduced after each heating cycle by centrifugation at 10ºC.

equilibrium is quickly reached, a significant amount of AuNPs was released after 4 cycles.

It is also worth to note that the more cycles exerted onto the MSN-DA-Au hybrid, the higher release (see Figures 7 and S8). This diverging behavior is of paramount importance for delivery applications as the *static* conditions (no medium replacement) may produce efficient cargo retention as most of the nanocaps remained at the hybrid, while the pulsating (*dynamic*) conditions, would produce a higher nanocap cleavage, and is expected to enhance cargo release. This effect could be seen on the TEM micrographs of the recovered hybrids after heating where it can be seen how the release mediated by dynamic conditions produced a greater release of AuNPs from the hybrids. (Figure 8) It is also important to emphasize that the small amount of AuNPs released at *static* conditions in periods up to 72h permit to discard other possible operating mechanisms such as silica dissolution, Diels-Alder adduct hydrolysis or thermal cleavage of the methyldisulfanyl:Au bond (see supporting information for experiments dealing which RS-SMe:Au bond strength).

Small molecule load and release experiments were performed by using a fluorophore model. As it is described in the experimental section, $(Ru(bipy)_3Cl_2)$ was loaded into MSN-MalGly following the same synthetic procedure: adduct formation, capping with AuNPs and final PEGylation. The successful preparation demonstrated that the loading step neither interfered on the adduct formation nor the AuNPs bonding.

The fluorophore release studies was tested under the *dynamic* conditions detailed previously. Those were accomplished in a continuous fluorometer employing conventional transparent polystyrene cuvettes for the measurements. Each cuvette was loaded with milli-Q water (3.5mL) and fitted to a Teflon cap consisting of a 150µL sample chamber loaded with the Ruthenium loaded, Au capped nanohybrid (Ru@MSN-DA-Au) suspension, closed with a dialysis membrane. This experimental configuration permitted to diffuse the released fluorophore through the membrane while the hybrid and the released AuNPs remained confined. The cuvettes were then externally heated at constant temperatures (37 and 65ºC) or under 10 minutes heating/cooling cycles between 37-65ºC as done previously for the *dynamic* Au release. The measurement of released the fluorescent probe under each tested condition is depicted in figure 9.

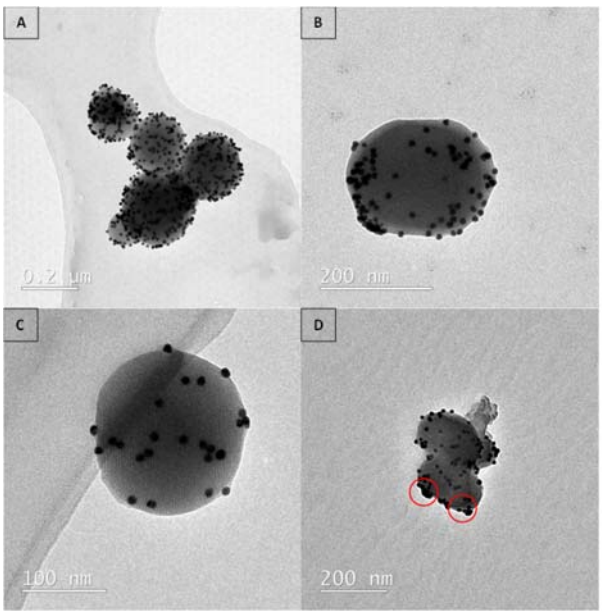

Figure 8: TEM micrographs of the different temperatures tested for the cyclic thermal treatment (10'/10'/25'/25') of the MSN-DA-Au hybrids. (A) 37ºC; (B and C) 65ºC and (D) 90ºC, here Au aggregation was observed.

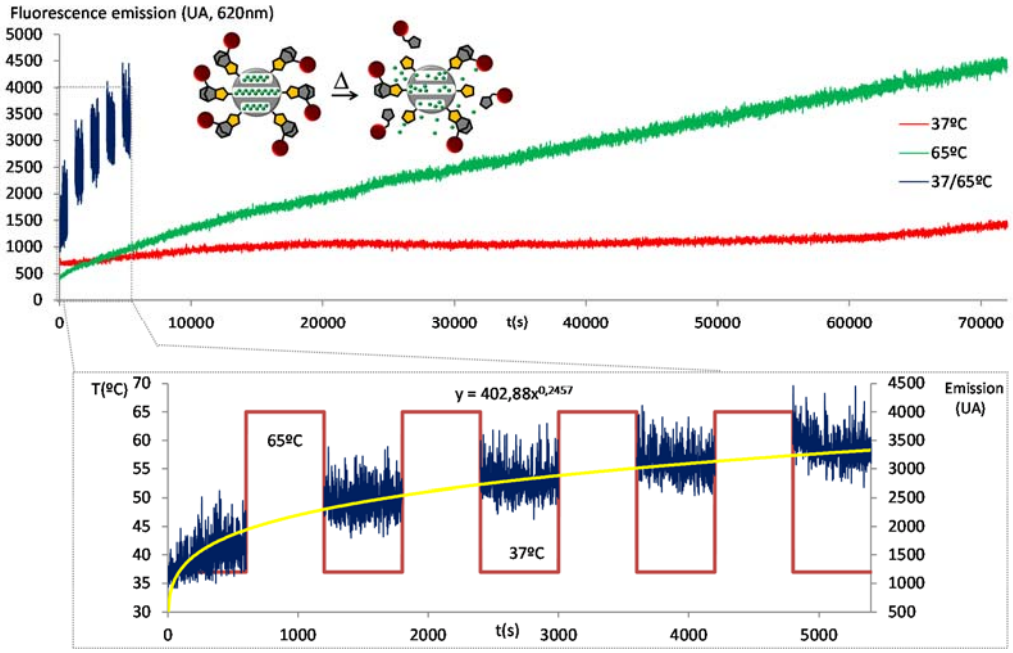

Figure 9: Comparative $Ru(bipy)_3Cl_2$ (λ_{ex}=452nm, λ_{em}=620nm) release studies from the loaded MSN-DA-Au under different thermal treatments. Red curve: release at constant 37ºC. Green curve: release at constant at 65ºC. Dark blue dashed curve: release at cyclic heating between 37 and 65ºC during 10 minutes intervals (for clarity fluorescence at 65ºC is not represented). Yellow curve: release extrapolation under cyclic thermal treatment. For a release graphic from a non cleavable system, please check figure S17).

$Ru(bipy)_3Cl_2$ release at constant temperatures of 37 or 65 °C showed a smooth release, indicating an effective retention of the model fluorophore within the MSNs. These values are in agreement with the high AuNPs retention observed under *static* thermal treatment. When the *dynamic* conditions were employed, an increased release of the fluorophore was obtained, in agreement with the greater cleavage of AuNPs obtained in previous experiments. Moreover, the system exhibited extraordinary retention at physiological temperature according to the basal release obtained at 37ºC during long periods of time (see Figure 9). This extraordinary retentive capacity suggests that an effective diffusion barrier is built on the pore outlets. We assume that this diffusion barrier is due to the rigidity of the Diels-Alder adducts (already observed in the N_2 adsorption isotherm experiment) together with the large size of the nanocaps and the presence of PEG chains bound to Au.

In order to prove that the claimed release properties were fully dependent on the retro Diels-Alder breakdown, the behavior of a modified Ru loaded MSN-Au hybrid connected with a non-cleavable linker was also evaluated. Figure S17 show that these hybrids do not produce fluorophore release even under thermal activation. Besides, the strength of the Diels-Alder-Au linkage throughout the RS-SMe:Au bond was also tested in an additional experiment with a non-cleavable methyldisulfanyl derivate (Figure S21). Thermal activation results of both non-cleavable hybrids showed AuNPs retention, seem to suggest that nanocap release is only operated through the proposed retro Diels-Alder mechanism.

The reported strategy is highly suitable for the preparation of therapeutically useful nanodevices with little synthetic effort. For instance, we were able to incorporate a vectorization agent by simply modifying the PEGylation step. The preparation of targeted hybrids was done employing a mixture of 10 mol% of thiolated

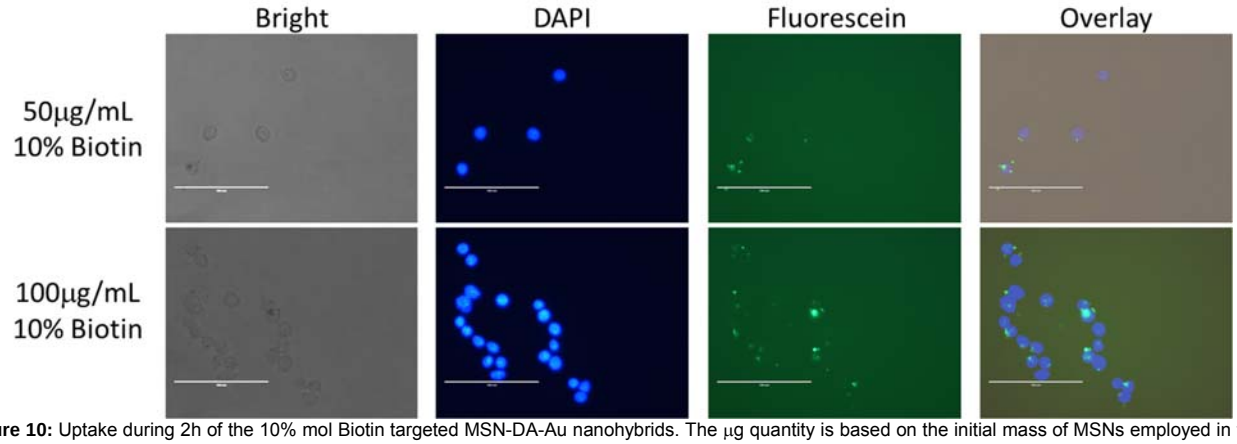

Figure 10: Uptake during 2h of the 10% mol Biotin targeted MSN-DA-Au nanohybrids. The µg quantity is based on the initial mass of MSNs employed in the synthesis. For this experiment, FITC-labelled MSNs (See Experimental Section) were employed. For experiments dealing with untargeted MSN-DA-Au hybrids please check figure S22.

PEG-Biotin (Supporting information) together with the stabilizing PEG-SH (90 mol%). The incorporation of targeting units onto the hybrids' surface was assessed by fluorescence microscopy experiments with MDA-MB-231 cell line (Figure 10).

The effective internalization achieved for the hybrid system with 10mol% of PEG-Biotin reveals two important aspects: first that the methodology of incorporation of the targeting ligand is adequate and second, that despite the low load of targeting ligand employed, there is an effective internalization of the hybrid. This last result is important too to demonstrate that thiol-containing compounds are not able to displace the Au:methyldisulfanyl bond; ensuring the integrity of the designed system and opening up the possibility of multi-ligand functionalization. Other advantage of the current design is that biotin could be employed as anchor point for the incorporation of more complex guidance systems throughout the avidin-streptavidin bridge.

To fully ensure the suitability of the system, were carried out too viability studies in presence of the prepared targeted hybrids. (Figure 11) These results indicate that concentrations up to 200 µg/mL only affect slightly the proliferation capacity of MDA-MB-231 (reduced in less than 15%). In fact, this also demonstrates the low toxicity of the hybrid system, which even at concentrations that greatly exceed the optimum concentration of work, do not show intrinsic toxicity.

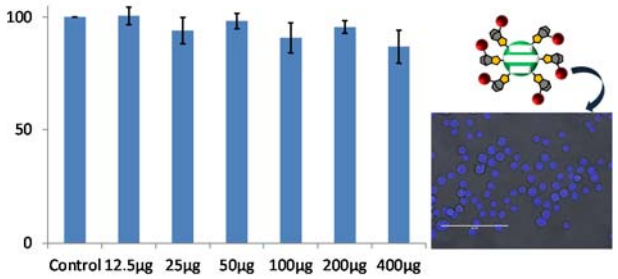

Figure 11: CellTiter 96® (MTS) cellular viability studies of the 10% targeted MSN-DA-Au-PEG-Biotin hybrids. Indicated quantities are referred to the initial mass of MSNs employed in the synthesis finally taken to 1mL of media. Cells represented are an actual image of the control experiment.

Conclusions

The development of nanomedicine has enabled the use of nanoparticles as drug delivery nanocarriers. Here, we describe a nanohybrid system formed by MSNs (with high loading capacity), with a Diels-Alder moiety as thermo-responsive linker and AuNPs as pore nanocaps. We have clearly demonstrated that Diels-Alder adducts are robust and temperature reversible linkers adequate to develop thermoresponsive nanohybrids. Furthermore, the claimed easy functionalization of the system was demonstrated by the use of PEG-Biotin as active targeting moiety. The *in vitro* results of internalization and viability against MDA-MB-231 cells demonstrate that this hybrid system shows high biocompatibility and can be used as a model for the development of highly efficient delivery systems. To this must be added the high capacity of retention and a good release profile showed when thermally treated activation; which is also relevant for the future development of drug nanocarriers. Moreover, although in this proof of concept the gold is round shaped and is not suitable for near infrared photoactivation. In future works this topic will be addressed to provide the system with a NIR light-induced response for the development of remotely triggerable devices.

Experimental Section

The following chemicals and reagents were purchased from Sigma-Aldrich: ammonium nitrate, cetyltrimethylammonium bromide (CTAB), tetraethyl orthosilicate (TEOS), fluorescein isothiocyanate (FITC), methylfurfuryldisulfide (MFD), tetrachloroauric acid 99.9%, 1-hydroxybenzotriazole (HOBt), HBTU, diisopropylethylamine (DIPEA), sodium citrate, $[Ru(bipy)_3]Cl_2$ and polyethyleneglycol derivates. From ABCR were obtained 3-aminopropyltriethoxysilane (APTES), 3-mercaptopropyltriethoxysilane (MPTES) and the NHS-modified biotin. Cell culture media DMEM, Fetal Bovine Serum and trypsin were purchased from Life Technologies; cell culture media Ham F12, PBS 10x and sodium pyruvate were purchased from Sigma-Aldrich and CellTiter 96® AQueous Assay from Promega. All compounds and solvents were employed without additional purification. Prepared materials were analyzed employing the available instruments: Philips X-Pert MPD diffractometer equipped with CuK_α radiation for X-ray diffraction (XRD), Perkin-Elmer Pyris Diamond TG/DTA analyzer for thermogravimetry and differential temperature analyses (TGA/DTA), Nicolet Nexus (Thermo Scientific) spectrometer equipped with a Smart Golden Gate ATR accessory for Fourier transform infrared (FTIR) spectra and a Bruker AV 250 MHz apparatus for liquid or a Bruker 400 MHz unit for solid NMR experiments. Freeze-dying was carried out in a Telstar LyoQuest apparatus. Particles' morphology was analyzed by transmission electron microscopy (TEM) was carried using a JEOL JEM 2100 or JEM 1400 microscopes equipped with a CCD camera (KeenView Camera). Pore properties were determined by N_2 adsorption isotherms on a Micromeritics ASAP 2020 instrument; the surface area was obtained by applying the Brunauer, Emmet & Teller (BET) method to the isotherm while pore size distribution was determined by the Barrett, Joyner & Halenda (BJH) method from the desorption branch of the isotherm. The zeta potential and hydrodynamic diameter of nanoparticles were measured by means of a Zetasizer Nano ZS (Malvern Instruments) equipped with a 633 nm laser. Ultraviolet-visible spectra were recorded in a Helios Zeta spectrometer from Thermo Scientific employing 1 cm optical way, reduced volume, disposable cuvettes. Fluorescence microscopy was performed on an Evos FL Cell Imaging System equipped with tree led channels (DAPI/GFP/RFP) from AMG (Advance Microscopy Group). Fluorescence spectrometry for release studies was performed in a PTI QuantaMaster 400 instrument from Horiba scientific, while for other fluorescence and absorbance measurements, a synergy 4 microplate reader from BioTek was employed.

Mesoporous Silica Nanoparticles. MSNs were synthesized employing a modified Stöber method from a mixture of APTES and TEOS (0.5/4.5 mL) which was dropwise (0.25 mL/min) added to a solution of 1 g of CTAB and 3.5 mL of NaOH (2 M) in 480 mL of bidistilled H_2O (Milli-Q) at 80ºC under vigorous stirring (600 rpm). Once the addition was concluded, the suspension obtained was further stirred keeping the temperature constant in order to finish the silica condensation. After 2 hours, the sample was centrifuged and washed with water and ethanol in order to remove the excess of reagents. Finally, the CTAB contained within the pores was removed by ionic exchange by using two reflux cycles with extracting solution of (10 g/L of NH_4NO_3 in 95:5 ethanol-water) for 2h. The particles were centrifuged and washed three times with EtOH and dried under vacuum. Fluorescein-labeled nanoparticles were synthesized using the a parallel protocol, but adding together with TEOS/APTES a previously reacted solution of 1mg FITC and 2.2 µL APTES in 100 µL ethanol for 2h. For the preparation of the thiol modified MSNs was employed MPTES in the synthesis.

Functionalization of MSNs with the Diels-Alder adduct (MSN-DA). For the preparation of the Diels-Alder functionalized MSNs (1.3 mmol NH_2/g MSN), a two-step protocol was employed in which the maleimidoglycine dienophile (2-(2,5-dioxo-2,5-dihydro-1H-pyrrol-1-yl)acetic acid) was first coupled to the amino groups. For this step, 500 mg of MSNs were reacted with 150 mg (0.97 mmol) of MalGly, 264 mg (1.9 mmol) of HOBt, 493 mg (1.3 mmol) of HBTU and 675 μL (3.9 mmol) of DIPEA in 50 mL of DMF for 8h. Once the reaction finished, the MSNs were centrifuged (9000 rpm, 10 min) and repeatedly washed with DMF until the reactants were completely removed (5 times). Finally MSN-MalGly were dispersed in 10 mL MeCN for the next step. The Diels-Alder adduct was formed by reacting 2 mL of the previous suspension of MSN-MalGly (≈ 100 mg) in MeCN with an excess (400 μL) of the chosen methylfurfuryldisulfide (MFD) diene at room temperature for 48 h. This reaction was placed in a rotatory shaker to provide an adequate mixture between the diene and MSN-DA. Once completed, MSN-DA were centrifuged (9000 rpm, 10 min, 10ºC) at low temperature and repeatedly washed with MeCN and EtOH until MFD was completely removed, finally were washed with Et_2O and dried under vacuum; storage was done refrigerated in tightly closed flasks.

Determination of adduct reversibility on MSN-DA by Thermogravimetric assays. For the determination of the Diels-Alder adduct reversibility, 2x5 mL suspensions of MSN-DA (3 mg/mL) in DMSO/H_2O (1:4) were prepared. Then, those samples were placed on tightly closed reaction vessels and placed on thermally stabilized baths with silicone oil 60 and 80ºC for 72h. After this time the sample was recovered by centrifugation (10000 rpm, 10 min), washed three times with EtOH and one with Et_2O. Finally the recovered MSNs were dried under vacuum, analyzed through thermogravimetry and compared with the precursor. In this case the incorporation of DMSO to the solvent mixture was crucial to obtain an adequate MSN-DA dispersibility and good solubility of the released MFD in the reaction media.

Synthesis of citrate stabilized Au Nanoparticles (AuNPs). The preparation of the AuNPs was done following the modified Turkevich methodology.[45] Briefly, in an *aqua regia* washed 1L rounded bottom flask fitted with a condenser was prepared a 500 mL of 1 mM $HAuCl_4$ solution in water under reflux. Then, 50 mL of 38.8 mM trisodium citrate were quickly added to the mixture, maintaining the reaction for 30 min. After cooling down the colloid was filtered through a 0.5 μm membrane filter and dialyzed throughout a 7000 Da cut off membrane in order to remove the excess of citrate and aggregates. The resulting Au colloid (10.9 nm) was stored refrigerated and protected from sunlight. ([AuNP] ≈ $1.59 \cdot 10^{-7}$ M, Supporting Information)

AuNPs deposition onto different functionalized Mesoporous Silica Nanoparticles. Preparation of MSN-Au hybrids was done according the following optimized protocol. A 1 mg/mL suspension of MSNs in DMF-H_2O (1:99) was dropwise added (1 mL/min) over AuNPs (2 mL per MSN milligram) under vigorous mechanical stirring and ultrasounds. Once the addition was completed, the mixture was allowed to react for 10 minutes maintaining both stirring and ultrasounds. Then, was added a solution of poly(ethylene glycol)methylether thiol (PEG-SH, MW=800) in water (10 μL per MSN milligram of a 10 mM PEG solution), stopping then the ultrasounds but keeping the stirring for additional 10 minutes. Finally, the reaction was treated with 30 μL/mg MSN-DA of a 5 M NaCl solution and maintained for additional 30 min. The silica-gold nanohybrids so obtained were collected by centrifugation (9000 rpm, 10 min, 10ºC) and washed with bidistilled water until remainder unbound gold was removed. To conclude, the obtained PEG coated MSN-Au hybrids were diluted with pure water in order to obtain a concentration of 10 mg/mL and were stored with refrigeration until use. For the preparation of 10 %mol biotin targeted devices, a mixture formed by 1 mM of the thiol-biotin bifunctional PEG (Supporting information) and 9 mM of PEG-SH was used.

Static thermal Au release from MSN-DA-Au. For these release experiments, 3x5 mL of 100 μg/mL samples of MSN-DA-Au were prepared in magnetically stirred, septum-capped, glass vials which were heated in thermally stabilized baths with silicone oil. The different measures were obtained from 1 mL aliquots taken from the reacted mixture at indicated times. The centrifugation at 9000 rpm for 10 min of each aliquot provided a supernatant composed by the released Au and a pellet that contained the remainder hybrid. The hybrid was then suspended to 1 mL with pure H_2O and recorded together with the supernatant between 400 and 800 nm. Absorbance values were used to determine the degree of release of the Au nanocaps.

Dynamic thermal induced Au release from MSN-DA-Au. These release experiments were performed employing 5 mL of a 100 μg/mL of hybrid suspension placed in thermally stabilized water baths during indicated periods. When completed, the components were separated by centrifugation (9000 rpm, 10 min) collecting the supernatants and dispersing the obtained pellet back to 5 mL with pure water; repeating iteratively this process for each temperature. Once the experiment was concluded the remainder hybrid was dispersed and analyzed through UV-Vis spectroscopy together with the supernatants.

Preparation of fluorophore loaded hybrids. The loading protocol started treating 100 mg of MSN-MalGly under vacuum and at 80ºC to ensure volatile compounds removal. Then, while in vacuum, 4 mL of a saturated solution of the fluorophore $Ru(bipy)_3Cl_2$ were injected in MeCN into the reaction vessel. The mixture was gently stirred for 24h at RT to permit the diffusion of the fluorophore throughout the mesopores. Then, the diene (MFD, 400 μL) was added to the mixture to produce the bulky Diels-Alder adduct at the pores' surface, the reaction was kept for 48h at RT. After the completion, the loaded particles were centrifuged and thoroughly washed with MeCN until excess of fluorophore and diene were removed. The particles were then washed with Et_2O, vacuum dried and stored refrigerated. The final capping with AuNPs was accomplished following the described protocol.

Fluorophore release studies were carried out in conventional disposable UV cuvettes fitted with a chamber containing cap in which were placed 150 μL of Ru@MSN-Au hybrids (5 mg/mL). Once loaded, the sample chamber was closed with a 7000 Da cut off dialysis membrane and placed in contact with the water filled cuvette (3.5 mL) allowing the diffusion of fluorophore. All fluorescence measurements were recorded under magnetic stirring to improve homogeneity. The different analysis were done under either constant (37ºC and 65ºC) for 72h or under cyclic heating/cooling cycles of 10 min between 37ºC (recording temperature) and 65ºC.

Cell viability and uptake assays. MDA-MB-231 cells were plated 24 h before starting the experiment in 12 well plates at a density of $2x10^5$ cells per well. The cytotoxicity of hybrids was evaluated using a commercial assay and following the manufacturer protocol. A common internalization procedure for both fluorescence microscopy analysis and viability studies was employed. The MSN-hybrid uptake by cells was done for the indicated concentrations prepared in culture media and in both cases, were performed over 2 h (n = 3). The cells destined to determine the viability were washed two times with PBS to remove non-internalized nanoparticles and were placed in 600 μL culture medium including MTS, maintaining the incubation for 3 h. Then, the medium was removed and its absorption at 490 nm was

measured using a microplate reader. In the other case, for fluorescence micrograph, the culture media and non-internalized nanohybrids were washed out and the cells were fixed with a methanol solution of DAPI for 2 min; followed by aspiration of the staining solution and washing with PBS before taking the micrographs.

Acknowledgements

The authors want to acknowledge financial support from European Research Council [ERC-2015-AdG-694160], Ministerio de Economía y Competitividad [MAT2015-64831-R] and the Centro de Investigación Biotecnológica en Red (CIBER) [CIB16-BM006]. SGG acknowledges the program Juan de la Cierva – Formación 2014 [FJCI-2014-2016].

Keywords: mesoporous silica, Silica-Au nanocomposites, mesopore reversible gating, Diels-Alder, targeting.

[1] A. C. Anselmo, S. Mitragotri, *AAPS J.* **2015**, *17*, 1041–1054.
[2] R. R. Castillo, M. Colilla, M. Vallet-Regí, *Expert Opin. Drug Deliv.* **2017**, *14*, 229–243.
[3] S. Gadde, *Med. Chem. Commun.* **2015**, *6*, 1916–1929.
[4] S. P. Hudson, R. F. Padera, R. Langer, D. S. Kohane, *Biomaterials* **2008**, *29*, 4045–4055.
[5] F. Tang, L. Li, D. Chen, *Adv. Mater.* **2012**, *24*, 1504–1534.
[6] J. Lu, M. Liong, Z. Li, J. I. Zink, F. Tamanoi, *Small* **2010**, *6*, 1794–1805.
[7] I. Izquierdo-Barba, M. Colilla, M. Manzano, M. Vallet-Regí, *Microporous Mesoporous Mater.* **2010**, *132*, 442–452.
[8] M. Vallet-Regi, A. Rámila, R. P. del Real, J. Pérez-Pariente, *Chem. Mater.* **2001**, *13*, 308–311.
[9] M. Vallet-Regí, F. Balas, D. Arcos, *Angew. Chem. Int. Ed. Engl.* **2007**, *46*, 7548–7558.
[10] Q. He, Y. Gao, L. Zhang, Z. Zhang, F. Gao, X. Ji, Y. Li, J. Shi, *Biomaterials* **2011**, *32*, 7711–7720.
[11] A. Baeza, M. Colilla, M. Vallet-Regí, *Expert Opin. Drug Deliv.* **2015**, *12*, 319–337.
[12] F. M. Veronese, G. Pasut, *Drug Discov. Today* **2005**, *10*, 1451–1458.
[13] A. S. Karakoti, S. Das, S. Thevuthasan, S. Seal, *Angew. Chemie - Int. Ed.* **2011**, *50*, 1980–1994.
[14] E. Aznar, M. Oroval, L. Pascual, J. R. Murguía, R. Martínez-Máñez, F. Sancenón, *Chem. Rev.* **2016**, *116*, 561–718.
[15] N. Song, Y.-W. Yang, *Chem. Soc. Rev.* **2015**, *44*, 3474–3504.
[16] F. Sancenón, L. Pascual, M. Oroval, E. Aznar, R. Martínez-Máñez, *ChemistryOpen* **2015**, *4*, 418–437.
[17] R. M. Fratila, S. G. Mitchell, P. del Pino, V. Grazu, J. M. de la Fuente, *Langmuir* **2014**, *30*, 15057–15071.
[18] T. Kuang, L. Chang, X. Peng, X. Hu, D. Gallego-Perez, *Trends Biotechnol.* **2016**, *0*, 3036–3055.
[19] E. Boisselier, D. Astruc, *Chem. Soc. Rev.* **2009**, *38*, 1759–1782.
[20] K. Wang, Z. Tang, C. J. Yang, Y. Kim, X. Fang, W. Li, Y. Wu, C. D. Medley, Z. Cao, J. Li, et al., *Angew. Chemie Int. Ed.* **2009**, *48*, 856–870.
[21] M. Hu, J. Chen, Z.-Y. Li, L. Au, G. V. Hartland, X. Li, M. Marquez, Y. Xia, *Chem. Soc. Rev.* **2006**, *35*, 1084-1094.
[22] P. K. Jain, K. S. Lee, I. H. El-Sayed, M. A. El-Sayed, *J. Phys. Chem. B* **2006**, *110*, 7238–7248.
[23] D. Kumar, N. Saini, N. Jain, R. Sareen, V. Pandit, *Expert Opin. Drug Deliv.* **2013**, *10*, 397–409.
[24] R. M. Cabral, P. V Baptista, *Expert Rev. Mol. Diagn.* **2014**, *14*, 1041–1052.
[25] F. Torney, B. G. Trewyn, V. S.-Y. Lin, K. Wang, *Nat. Nanotechnol.* **2007**, *2*, 295–300.
[26] J. Zhu, M.D. Ganton, M.A. Kerr, M. S. Workentin, *J. Am. Chem. Soc.* **2007**, *129*, 4904–4905.
[27] J. Zhu, B. M. Lines, M.D. Ganton, M.A. Kerr, M. S. Workentin, *J. Org. Chem.* **2008**, *73*, 1099–1105.
[28] J. Zhu, A. J Kell, Workentin M. S., *Org. Lett.* **2006**, *8*, 4993–4996.
[29] S. Ghiassian, P. Gobbo, M. S. Workentin, *Eur. J. Org. Chem.* **2015**, *24*, 5438–5447.
[30] D. R. Radu, C. Y. Lai, K. Jeftinija, E. W. Rowe, S. Jeftinija, V. S. Y. Lin, *J. Am. Chem. Soc.* **2004**, *126*, 13216–13217.
[31] J. L. Vivero-Escoto, I. I. Slowing, C.-W. Wu, V. S.-Y. Lin, *J. Am. Chem. Soc.* **2009**, *131*, 3462–3463.
[32] G. Luo, W. Chen, H. Jia, Y. Sun, H. Cheng, R. Zhuo, X. Zhang, *Nano Res.* **2015**, *8*, 1893–1905.
[33] R. Zhang, L. Li, J. Feng, L. Tong, Q. Wang, B. Tang, *ACS Appl. Mater. Interfaces* **2014**, *6*, 9932–9936.
[34] R. Liu, Y. Zhang, X. Zhao, A. Agarwal, L. J. Mueller, P. Feng, *J. Am. Chem. Soc.* **2010**, *132*, 1500–1501.
[35] W. Gao, W. Cao, Y. Sun, X. Wei, K. Xu, H. Zhang, B. Tang, *Biomaterials* **2015**, *69*, 212–221.
[36] Y.-L. Liu, T.-W. Chuo, *Polym. Chem.* **2013**, *4*, 2194-2205.
[37] N. Roy, B. Bruchmann, J.-M. Lehn, *Chem. Soc. Rev.* **2015**, *44*, 3786–3807.
[38] A. Gandini, *Prog. Polym. Sci.* **2013**, *38*, 1–29.
[39] R. Tong, L. Tang, L. Ma, C. Tu, R. Baumgartner, J. Cheng, *Chem. Soc. Rev.* **2014**, *43*, 6982–7012.
[40] T. Engel, G. Kickelbick, *Chem. Mater.* **2013**, *25*, 149–157.
[41] S. Schäfer, G. Kickelbick, *Polymer (Guildf).* **2015**, *69*, 357–368.
[42] B. Rühle, S. Datz, C. Argyo, T. Bein, J. I. Zink, *Chem. Commun.* **2016**, *52*, 1843–1846.
[43] P. K. Jain, K. S. Lee, I. H. El-Sayed, M. A. El-Sayed, *J. Phys. Chem. B*, **2006**, *110*, 7238–7248.
[44] L. M. Liz-Marzán, *Langmuir*, **2006**, **22**, 32–41
[45] K. C. Grabar, R. G. Freeman, M. B. Hommer, M. J. Natan, *Anal. Chem.* **1995**, *67*, 735–743.

FULL PAPER

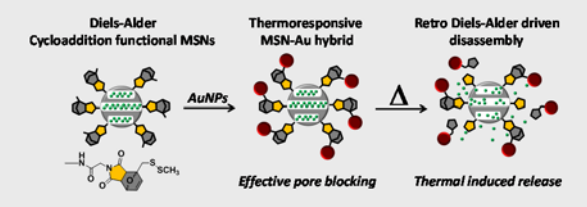

The use of Diels-Alder cycloadducts as thermoresponsive fragments in combination with Au nanocaps proved to generate efficient and triggerable nanogates onto silica mesopores that also are willing to be modified with vectorization agents easily.

Rafael R. Castillo, David Hernández-Escobar, Sergio Gómez-Graña, María Vallet-Regí**

Page No. – Page No.

Reversible nanogate system for Mesoporous Silica Nanoparticles based on Diels-Alder adducts